Rev. Adv. Mater. Sci. 31 (2012) 47-53

DIRECT AND REVERSE MARTENSITIC TRANSFORMATION AND FORMATION OF NANOSTRUCTURED STATES DURING SEVERE PLASTIC DEFORMATION OF METASTABLE AUSTENITIC STAINLESS STEEL

I. Yu. Litovchenko[1], A. N. Tyumentsev[1,2], M. I. Zahozheva[2] and A. V. Korznikov[3]

[1]Institute of Strength Physics and Materials Science SB RAS, pr. Akademicheskii, 2/4, Tomsk, 634021, Russia.
[2]Tomsk State University, pr. Lenina , 36, Tomsk, 634050, Russia
[3]Institute for Metals Superplasticity Problems RAS, ul. St. Khalturina 39, Ufa, 450001, Russia

Received: April 20, 2012

Abstract. The deformed structure features and phase composition changes of austenitic stainless steel after severe plastic deformation by rolling and high pressure torsion in Bridgman's anvils are studied using transmission electron microscopy, X-ray diffraction and magnetization measurement techniques. It is shown that during severe plastic deformation by high pressure torsion not only direct ($\gamma \rightarrow \alpha'$) but also reverse ($\alpha' \rightarrow \gamma$) martensitic transformations occur, which is revealed by the changes in the volume content of α' - martensite during deformation. Based on the results obtained, the mechanisms of phase transformations and nanostructured states formation are discussed.

1. INTRODUCTION

It is known that under conditions of severe plastic deformation (SPD) of metastable austenitic steels we observe direct ($\gamma \rightarrow \alpha'$) and ($\gamma \rightarrow \varepsilon$) martensitic transformations (MTs) [1-3]. They to a large extent determine the features of the deformed structure and phase composition of submicron and nanocrystalline (SMC and NC) austenitic steels, obtained by SPD.

In a recent work [4] the authors showed that under the SPD condition metastable austenitic steels undergo not only direct ($\gamma \rightarrow \alpha'$), but also reverse ($\alpha' \rightarrow \gamma$) MTs. In particular based on the X-ray diffraction (XRD) data they reported that after High Pressure Torsion (HPT) of steel 304 at a rate of up to 5 rpm nearly 100% α' - martensite is formed in the initial stage of deformation. Then its volume fraction decreases to ~ 20%, with a further increase to 50%. The authors attribute the reverse MT to the increasing temperature. According to the in-situ measurements by a thermocouple it increased to 200 °C.

Earlier in our works [5,6], we suggested that under SPD direct and reverse ($\gamma \rightarrow \alpha \rightarrow \gamma$) martensitic transformations occur in austenitic steels. Note that the reverse transformation in this case follows an alternative path. We showed that this is one of the mechanisms of formation of fragments of localized deformation bands (LDBs) - a type of shear bands with high-angle misorientations close to $\approx 60°$<110>, $\approx 35°$<110>, and $\approx 50°$<110>, and thus one of the mechanisms of formation of SMC and NC structural states in austenitic steels.

In this work we investigate deformed structure evolution and phase transformations in metastable austenitic steel under SPD by rolling and HPT treatment. To prove experimentally direct and reverse martensitic transformations under severe plastic deformation we study the changes in the volume

Corresponding author: Igor Yu. Litovchenko, e-mail: litovchenko@spti.tsu.ru

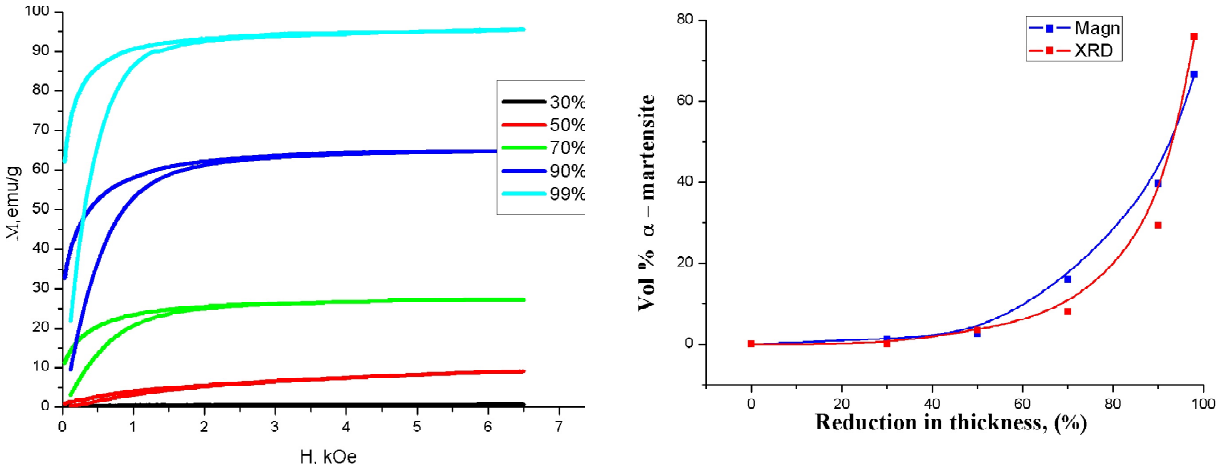

Fig. 1. Changes in volume content of α´ - martensite during rolling deformation. (*a*) - Specific magnetization vs. magnetic-field strength for different degrees of rolling deformation, (*b*) – Volume % of α´ - martensite vs. degree of rolling deformation by XRD and magnetic measurements.

fractions of γ and α´ phases and detect reorientation fragments of γ and α´ phases that evidence of direct and reverse martensitic transformations. We investigate the mechanisms of deformation and crystal lattice reorientation during formation of SMC and NC structural and phase states.

2. EXPERIMENTAL PROCEDURE

For the investigation, we used a chromium–nickel metastable austenitic steel Fe–18%Cr–8%Ni-Ti. Prior to deformation the samples were annealed at 1100 °C for 1 hour and then quenched in water. In the initial state the volume content of austenite is about 100% according to the X-ray diffraction data. The plastic deformation by rolling was performed at room temperature to $\varepsilon \leq 99\%$. The initial and final specimen thicknesses were 12 and 0.12 mm, respectively. The samples for HPT in Bridgman anvils were shaped as disks ≈ 0.2 mm thick and 8 mm in diameter. Their deformation was achieved at a pressure of ~8 GPa within the values of N = 0.1 to 8 turns of anvil, which corresponded to the true logarithmic strain e = 2.5 – 6.9. The rate of loading was below 1 rpm to prevent significant overheating of the samples. The specimen temperature during HPT was measured by a thermocouple located in the lower anvil at a distance of 0.7 mm from the specimen surface. At the speed of rotation used the temperature did not exceed 60 °C.

The electron-microscopic investigations were conducted using the Philips CM-12, Philips CM-30, and JEOL-2100 electron microscopes at an accelerating voltage of 120, 300, and 200 kV, respectively. The thin foils were prepared from sections parallel and perpendicular to the rolling plane and the plane of the anvil by the electropolishing with the use of planar stainless-steel electrodes in an electrolyte containing 450 ml of orthophosphoric acid, 50 g of chromic anhydride, and 2 ml of hydrogen peroxide at a current density of ≈ 2.4 A/cm^2. Thin foil for cross-sections samples were cut at a distance of half the radius of the sample.

The changes in the phase content in the process of deformation were additionally studied by X-ray diffraction using the Shimadzu XRD-6000 and DRON-7 «Burevestnik» diffractometers. To determine the volume content of the magnetic phase, we employed the method of measuring specific magnetization depending on the magnetic-field strength in an N-04 Magnetometer [7]. Since among the possible phases (γ, ε, α') only α' phase possesses ferromagnetism, the resulting curves of specific magnetization versus the magnetic-field strength were converted to the volume content of the α'- phase. The value of the saturation magnetization 154 emu/g, which corresponds to the 100% α' – martensite, was taken from [8].

3. RESULTS

The X-Ray diffraction and electron microscopy studies of the phase composition of the material after deformation have shown that plastic deformation leads to a direct ($\gamma \rightarrow \alpha'$) phase transformation and formation of structural and phase inhomogeneities at the meso- and microscale levels. We observed the regions with prevailing austenite, martensite and two-phase regions. We attribute the differences in the structure and phase states to the local varia-

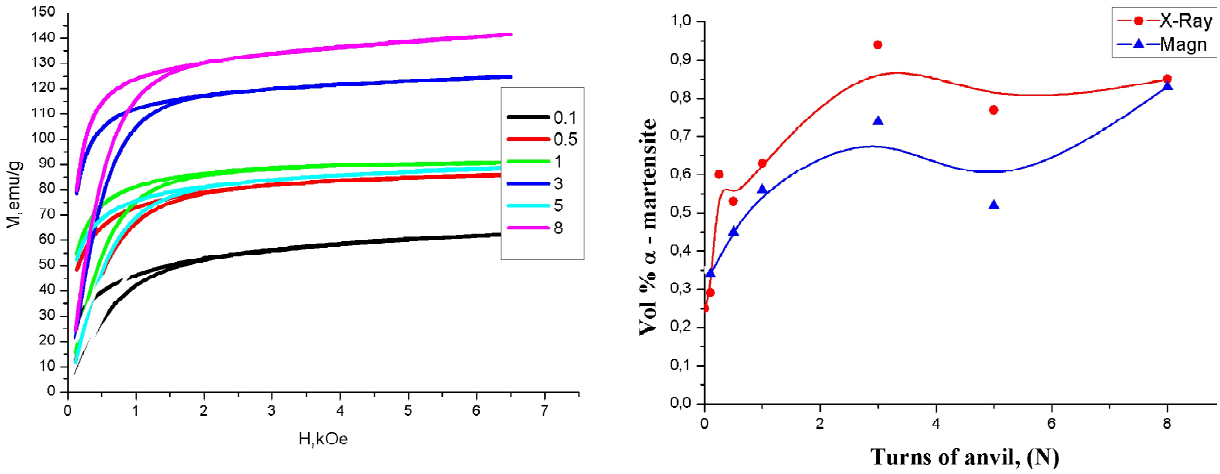

Fig. 2. Changes in volume content of α´ - martensite during HPT deformation. (*a*) - Specific magnetization vs. magnetic-field strength for different turns of anvil (*N*), (*b*) – Volume % of α´ - martensite vs. number of anvil turns (*N*) by XRD and magnetic measurements.

tions in the volume content of α´-martensite. According to the X-ray diffraction analysis, there is no ε - martensite in the deformed samples. The electron-microscopic investigations have shown a small amount of ε - martensite in a form of thin plates both in the case of rolling deformation and HPT. Since this phase is not detected by X-ray diffraction, its volume fraction does not exceed ~1%.

3.1. XRD and magnetic measurements

Fig. 1a shows the magnetization plotted as a function of the magnetic field, the reduction in the specimen thickness after deformation being from 30 to 99%. The as-received specimens exhibit negligibly small magnetization. Based on the M(H) dependences at different degrees of deformation we constructed a curve of the magnetic-phase content versus the degree of deformation by rolling. Fig. 1b shows the dependence of the volume content of α´-martensite on the degree of deformation by rolling, obtained by X-ray diffraction and magnetic measurements. It is clear that the volume content of α´-martensite increases with increasing strain and reaches ≈70-80% for the rolling deformation is ε = 99%. There are some differences in the volume content of martensite obtained by XRD and magnetic measurements. We attribute them to the local variations in the volume content of α´-martensite.

The behavior of the volume content of martensite in the case of HPT is different. Fig. 2a shows the dependences of the specific magnetization on the magnetic-field strength for different turns of anvil (*N*). Fig. 2b represents the graphs of the volume content of α´-martensite versus the degree of deformation by HPT obtained from the XRD data and magnetic measurements. We see that the volume fraction of α´-martensite increases with increasing strain and reaches 70-95% for *N* = 3 turns of anvil, then it declines to 50-75% with subsequent increase to 80% for *N* = 8. A decrease in the volume content of α´-martensite during SPD by torsion suggests that not only the direct ($\gamma \rightarrow \alpha'$), but also reverse ($\alpha' \rightarrow \gamma$) martensitic transformations take place in this case.

3.2. Electron-microscopy study

The electron-microscopic studies have shown that α´-martensite is formed in the deformed structure consisting of deformation microtwins and localized deformation bands (LDBs) the shear band type. Fig. 3 shows a typical deformed structure of the steel after rolling deformation to 70%. Characteristic elements of the deformed structure are presented by its dark-field images in the corresponding reflections (Figs. 3c-3e) and in the scheme (Fig. 3b). From the analysis of dark-field images and SAD pattern follows that a fragment of LDB with reorientation of ~ 60° <110> is formed in the microtwinning structure and is surrounded by α´-martensite plates. Formation of these fragments can be accounted for by direct and reverse martensitic transformations, with reverse transformation following an alternative path [5,6]. Here, we for the first time observed the fragments of ~ 60° <110> reorientation in austenite together with plates of α´-martensite.

Fig. 4 illustrates the prevailing austenitic regions after deformation by rolling to 98%. In the SMC grains of austenite we observed characteristic banded con-

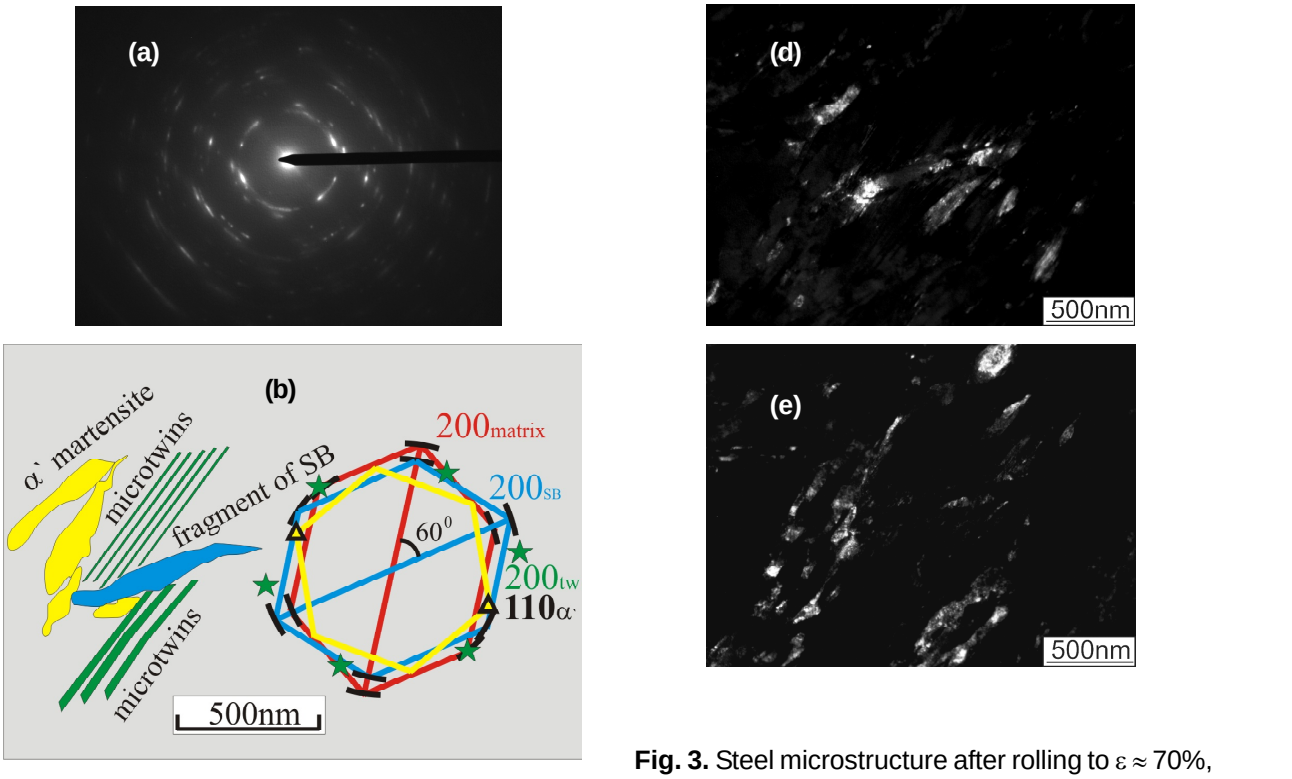

Fig. 3. Steel microstructure after rolling to $\varepsilon \approx 70\%$, (*a*) - SAD pattern, (*b*) - a schematic of the SAD pattern and deformed structure elements, (*c*) - DF image in g = (111) γ - matrix, (*d*) - DF image in g = (111) γ – shear band (SB), the matrix reflection g = (200) γ partially contributes to the formation of the DF image and (*e*) - DF image in g = (110) α' – martensite.

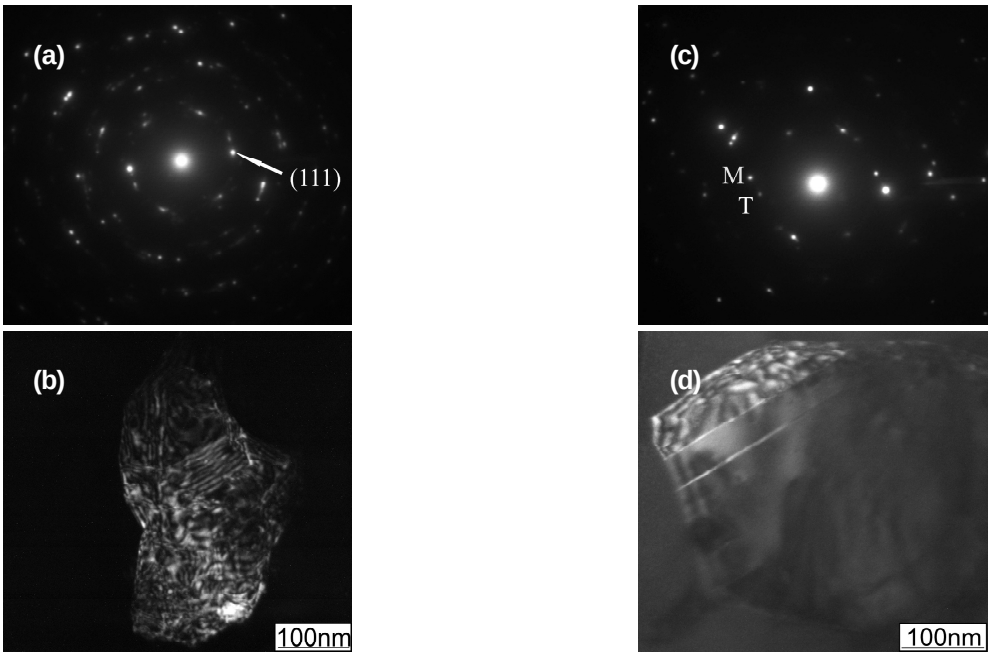

Fig. 4. Deformed structure of prevailing austenitic regions after $\varepsilon \approx 98\%$ of rolling deformation. (*a*) – SAD pattern from grain with banded contrast, (*b*) – DF image in g = (111) γ from grain with banded contrast, (*c*) - SAD pattern from grain with dynamic recrystallization and a nanotwin; T and M are the twin and matrix reflections, respectively, (*d*) - DF image in g = (111) γ –twin.

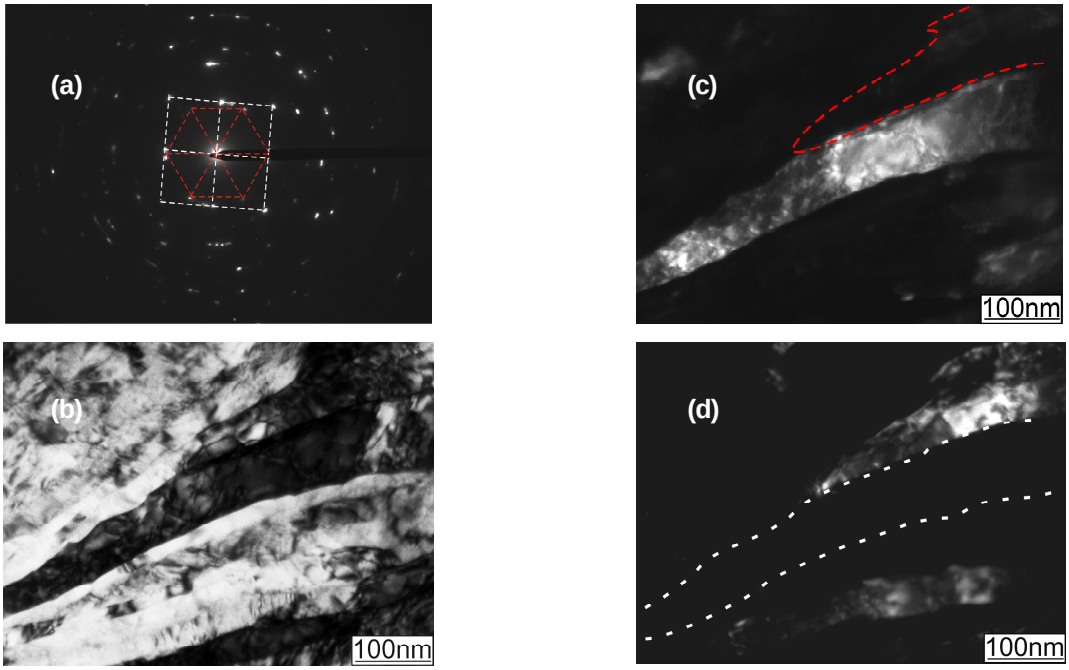

Fig. 5. Deformed structure of prevailing martensitic regions after $\varepsilon \approx 90\%$ of rolling deformation. (*a*) – SAD pattern from lamella structure with sketch of two zone axes [001] – white dash lines, [111] - red dash lines, with joint reflection g = ($\bar{1}$ 10), (*b*) – BF image of lamella structure, (*c*) - DF image in g = (110) α' of [001] zone axe, with sketch of adjacent lamella, and (*d*) - DF image in g = ($\bar{1}$ 01) α' of [111] zone axe, with sketch of adjacent lamella.

trast (Fig. 4b*)*, which can be associated with the internal dislocation structure, low-angle boundaries of misorientation, and/or inclined defects (stacking faults and twin boundaries). Inside some SMC grains of austenite we see the regions of dynamic recrystallization and nanotwins (Fig. 4d).

A different defect structure is observed in the prevailing martensitic regions. There are lamella banded structures with low- and high-angle misorientations. TEM analyses of dark-field images and SAD pattern from the lamella structure (Fig. 5) have shown that we have two zone axes of BCC [001] and [111] with a joint reflection g = ($\bar{1}$ 10). These zone axes are indicated with white and red dashed lines in Fig. 5a and the corresponding dark-field images. The crystal lattice misorientation between these two marked lamella is close to ~ 60° <110>. We suppose that these misorientations in the martensite can be produced via ($\alpha' \rightarrow \gamma \rightarrow \alpha'$) MTs, where the reverse transformation follows an alternative path. Inside the martensitic lamella the dislocations density is quite high.

The deformed structure in the initial stages of deformation by torsion (from 0.1 to 3 turns) is similar to that after deformation by rolling to 90-99%. We see the regions with the prevailing austenite, martensite, and two phase regions. The austenitic regions are presented by deformation twins in one or more twinning systems and LDBs. There are lamella banded structures with high- and low-angle misorientations in the martensitic regions.

Fig. 6 shows the deformed structures of the steel after deformation by HPT from 1 to 8 turns. From the qualitative analyses of dark-field images and SAD patterns it follows that in the initial stages of deformation (up to 3 turns) the volume fraction of martensite is much larger than that of austenite. After 5 turns the volume fractions of the phases are approximately equal, while after 8 turns the volume content of martensite increases again.

4. DISCUSSION

From the results obtained by XRD and magnetic studies it follows that in the case of rolling a monotonic increase in the martensitic phase content of deformation is observed. In the case of HPT, on the other hand, we see a nonmonotonic dependence of the martensite content on the degree of deformation. A decreased volume content of martensite after 5 turns of the anvil is an experimental proof of a reverse ($\alpha' \rightarrow \gamma$) martensitic transformation. These results are qualitatively confirmed by the electron microscopy data. In addition a TEM analysis re-

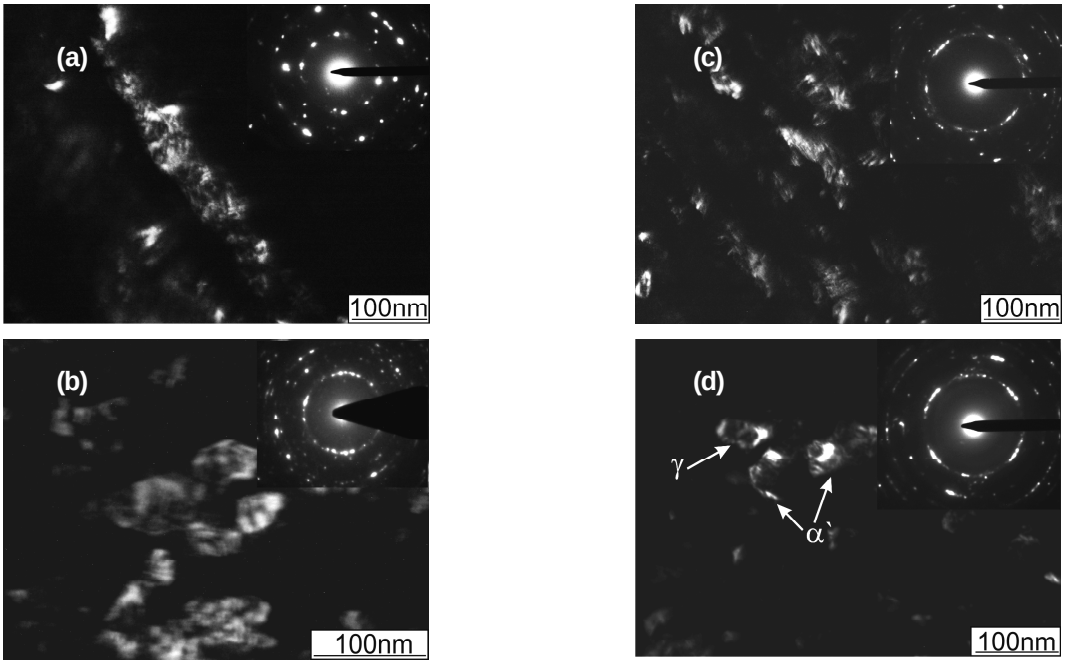

Fig. 6. TEM images of steel microstructure after HPT. (*a*) – DF image in g = (110) α' and corresponding SAD pattern, 1 turn of anvil, (*b*) –DF image in g = (110) α' and corresponding SAD pattern, 3 turns, (*c*) - DF image in g = (111) γ and corresponding SAD pattern, 5 turns, and (*d*) - DF image in joint g = (110) α' + g = (111) γ and corresponding SAD pattern, 8 turns.

veals the presence of a specific misorientation, i.e. ~ 60°<110> in austenite. According to [4,5], in the case of the Kurdyumov-Sachs orientation relationships this misorientation in austenite can be produced by ($\gamma \rightarrow \alpha' \rightarrow \gamma$) direct and reverse martensitic transformations where the reverse transformation follows an alternative path. So we think that a decreasing volume content of martensite in the course of SPD by HPT together with the existence of specific misorientations of crystal lattice in the austenite provide an experimental evidence of abovementioned direct and reverse martensitic transformations in the experimental steel specimens.

After a further increase in strain by HPT (more then 5 turns of anvil) the following increase in the volume content of martensite is observed. This implies that retained or reverted austenite is again transformed in to martensite. Besides this, we see some specific misorientations, i.e. ~ 60° <110> in martensite. In [9] it was shown that this misorientation in martensite may result from ($\alpha' \rightarrow \gamma \rightarrow \alpha'$) martensitic transformations. In our case of HPT, we can not rule out the possibility of these transformations.

Based on the traces of ε - martensite observed for all of the investigated degrees of deformation and literature data [1-3] on the role of ε -martensite as an intermediate phase in the course of SPD of austenitic steels, we can assume a more complicated character of phase transformations, i.e. $\gamma \rightarrow \varepsilon \rightarrow \alpha'$ ($\gamma \rightarrow \varepsilon \rightarrow \alpha' \rightarrow \gamma$), *etc*.

The specimen heating during the HPT process depends on the speed of rotation. In our case, there was no significant increase in the temperature of the specimen as a whole in the course of plastic deformation. However, we do not rule out that in certain local areas in the process of deformation the temperature did exceed 60 °C. We believe the fields of high local stresses and their gradients generated in the course of SPD by HPT in the SMC and NC martensitic structure with high dislocation density to be the major causes of reverse transformation. In the course of continuous plastic deformation in the SMC and NC martensitic structure in the case of a favorable geometry, the fields of local stresses give rise to reverse martensitic transformation. Thus we can conclude that it is the locally increased temperature and high hydrostatic pressure in the deformation process that contribute to the reverse transformation.

Similar reverse transformation from bcc to fcc structure was also reported [10] during HPT of carbon steel at room temperature. It has been proposed that the driving force for this reverse martensitic transformation is provided by the Gibbs free energy of ultra-fine bcc grains together with very high shear

stresses [10]. In the case of austenitic steel, we assume the same reasons for the reverse transformation.

In the case of rolling up to 99% the inhomogeneous structure and phase states with fragments of SMC and NC scale are being formed in the steel. HPT up to 8 turns (e = 6.9) leads to a more homogeneous structure, consisting of fragments of two phases, with an average size being less than 100 nm.

According to the TEM studies, high-angle misorientation boundaries of the SMC and NC structures of austenite are formed by deformation twinning and intense shear strain in the LDBs (shear band type). The high-angle misorientation boundaries in the SMC and NC martensite structure are formed by different variants of $\gamma \rightarrow \alpha'$ transformation. We also believe that these boundaries in martensite and austenite are formed with the participation of direct and reverse martensitic transformations. A wide range of low-angle misorientation boundaries of austenite and martensite is associated with the dislocation-disclination deformation and crystal lattice reorientation.

5. SUMMARY

It has been shown that during SPD of the metastable austenitic steel by HPT not only direct ($\gamma \rightarrow \alpha'$) but also reverse ($\alpha' \rightarrow \gamma$) MTs occur, which is revealed by the changes in the volume content of martensite during deformation. We have observed the fragments of misorientations in the austenite and martensite with disorientation of ~ 60° <110>, which also favor the direct and reverse martensitic transformations in the course of SPD of the experimental steel specimens. During SPD of metastable austenitic steel, two-phase SMC and NC structural states are formed. The mechanisms of their formation are mechanical twinning and formation of LDBs in austenite, direct and reverse martensitic transformations, as well as dislocation-disclination deformation and crystal lattice reorientation.

REFERENCES

[1] C.X. Huang, G. Yang, B. Deng, S.D. Wu, S.X. Li and Z.F. Zhang // *Phil. Mag.* **87,31** (2007) 4949.

[2] S.S.M. Tavares, D. Gunderov, V. Stolyarov and J.M. Neto // *Mater. Sci. Engng* **A 358** (2003) 32.

[3] E. Nagy, V. Mertinger, F. Tranta and J. Sólyom // *Mater. Sci. Engng A* **378** (2004) 308.

[4] J.G. Li, M. Umemoto, Y. Todaka, K. Fujisaku and K. Tsuchiya // *Rev. Adv. Mater. Sci.* **18** (2008) 577.

[5] A.N. Tyumentsev, I.Yu. Litovchenko, Yu.P. Pinzhin, A.D. Korotaev, N.S. Surikova, S.L. Girsova and V.A. Nesterenkov // *Phys. Met. Metallogr. Vol*. **95(2)** (2003) 86.

[6] A.N. Tyumentsev, I.Yu. Litovchenko, Yu.P. Pinzhin, A.D. Korotaev, S.L. Girsova and V.A. Nesterenkov // *Phys. Met. Metallogr. Vol*. **95(3)** (2003) 88.

[7] V.Yu. Kreslin and E.P. Naiden // *Instrum. Exp. Techn*. **45** (2002) 55.

[8] K. Mumtaz, S. Takahashi, J. Echigoya, Y. Kamada, L.F. Zhang, H. Kikuchi, K. Ara and M. Sato // *Journal of Materials Science* **39** (2004) 85.

[9] I.G. Kabanova and V.V. Sagaradze // *Phys. Met. Metallogr. Vol*. **88(2)** (1999) 143.

[10] Yu. Ivanisenko, I. MacLaren, X. Sauvage and H.–J. Fecht // *Acta mater*. **54** (2006) 59.